11-1996

Performance of CdZnTe strip detectors as sub-millimeter resolution imaging gamma radiation spectrometers

M Mayer
University of New Hampshire - Main Campus

V Boykin
University of New Hampshire - Main Campus

M L. Cherry
Louisiana State University - Baton Rouge

J F. Courville
University of Montreal

F P. Doty
DIGIRAD

See next page for additional authors

Recommended Citation

Mayer, M.; Boykin, D.V.; Cherry, M.L.; Courville, J.F.; Doty, F.P.; Drake, A.; Guzik, T.G.; Hamel, L.A.; Larson, K.; Macri, J.R.; McConnell, M.L.; Ryan, J.M.; Tousignant, O., "Performance of CdZnTe strip detectors as sub-millimeter resolution imaging gamma radiation spectrometers," Nuclear Science Symposium, 1996. Conference Record., 1996 IEEE , vol.2, no., pp.830,834 vol.2, 2-9 Nov 1996.

Performance of CdZnTe Strip Detectors as Sub-millimeter Resolution Imaging Gamma Radiation Spectrometers

M. Mayer[1], D.V. Boykin[1], M.L. Cherry[3], J.F. Courville[2], F.P. Doty[4], A. Drake[1], T.G. Guzik[3], L.A. Hamel[2], K. Larson[1], J.R. Macri[1], M.L. McConnell[1], J.M. Ryan[1], O. Tousignant[2]

[1] Space Science Center, University of New Hampshire, Durham, NH 03824 USA
[2] Department of Physics, University of Montreal, Montreal, H3C 3J7, Canada
[3] Department of Physics and Astronomy, Louisiana State University, Baton Rouge, LA 70803 USA
[4] DIGIRAD, San Diego, CA 92121-2410 USA

Abstract

We report γ-ray detection performance measurements and computer simulations of a sub-millimeter pitch CdZnTe strip detector. The detector is a prototype for γ-ray astronomy measurements in the range of 20–200 keV. The prototype is a 1.5 mm thick, 64 × 64 orthogonal stripe CdZnTe detector of 0.375 mm pitch in both dimensions, with approximately one square inch of sensitive area. Using discrete laboratory electronics to process signals from an 8 × 8 stripe region of the prototype we measured good spectroscopic uniformity and sub-pitch (~ 0.2 mm) spatial resolution in both *x* and *y* dimensions. We present below measurements of the spatial uniformity, relative timing and pulse height of the anode and cathode signals, and the photon detection efficiency. We also present a technique for determining the location of the event in the third dimension (depth). We simulated the photon interactions and signal generation in the strip detector and the test electronics and we compare these results with the data. The data indicate that cathode signal—as well as the anode signal—arises more strongly from the conduction electrons rather than the holes.

I. INTRODUCTION

Sub-millimeter resolution CdZnTe position-sensitive detector technology is a strong prospect for achieving both improved energy and spatial resolution with high stopping power and without the need for cryogenic cooling [1, 2, 3, 4, 5, 6]. The operating principles of CdZnTe strip detectors are described in ref. [4]. A major goal of the efforts is the development of large area imaging modules incorporating strip detectors and the associated electronics in compact packages.

Demonstrations of the spectroscopic and imaging properties of prototype CdZnTe strip detectors have been a focus of much of this work [1, 2, 4]. Modeling of the photon interaction, charge transport and signal generation in these detectors is also important [7, 8, 9, 10]. Achieving agreement between simulations and prototype measurements will be a significant development milestone. Accurate modeling will help specify optimum detector geometries and appropriate signal processing electronics, thus minimizing the number of expensive and time consuming hardware prototypes.

0-7803-3534-1/97 10.00

II. PROTOTYPE STRIP DETECTOR DESCRIPTION AND TEST SETUP

The prototype detector was manufactured by DIGIRAD [1]. A pattern of 64 × 64 interdigitated and orthogonal contact stripes on each surface defines a 24 mm × 24 mm imaging area (5.76 cm^2) on a 28 mm × 28 mm CdZnTe substrate that is 1.5 mm thick. The stripe pitch is 0.375 mm with a 0.15 mm gap between stripe contacts.

Figure 1 illustrates the laboratory setup for the prototype strip detector measurements. Independent ac-coupled signal channels for each of 8 consecutive stripes in each dimension define a 3 mm × 3 mm active test region of 64 "pixels," i.e. 1/64 of detector's area. Amptek A225 preamp/shaper circuits and additional op amps provide fast (200 ns rise time) signals for level discrimination and coincidence logic and slow (2 μs) channels for pulse height measurements on each stripe. All stripes on each detector surface are biased to assure a uniform electric field in the CdZnTe. The load resistance is 1 GΩ. Any *x*-*y* discriminator coincidence triggers the readout of 17 parameters for each event: 16 pulse heights and the relative arrival time of coincident anode and cathode signals. The detector and test electronics are packaged so that the detector can be illuminated from either surface. The typical bias used for these measurements is 200 V. All measurements were performed at room temperature.

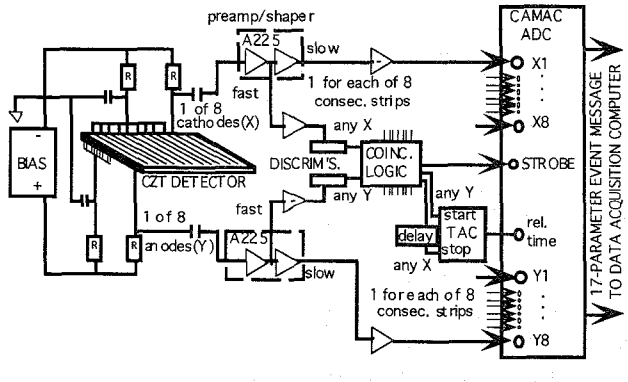

Figure 1. Test setup (orthogonal stripe coincidence mode)

III. SIMULATION MODEL

The model is intended to be an end-to-end tool for simulating all detection and measurement processes from

photon interaction to the electronics. The detector material (mobilities, trapping and detrapping coefficients), bias, and geometry (thickness, electrode pitch and gap) of the prototype detector are represented in the model. A GEANT module simulates the photon interaction locations, the energy deposit and the distribution of the ionization charges for incident photons of any given energy. A charge transport and signal generation module [7, 9, 10] computes the signal induced on any electrode for photon interaction locations at any depth below the electrode or at any lateral position between electrodes. The model also simulates the charge signal processing of the fast and slow channels of the laboratory test electronics. The pulse heights and relative timing of these processed signals can be histogrammed for comparison with the laboratory data.

IV. Test and Simulation Results

A. *Spectroscopy (anodes)*

It has been demonstrated that signal charge for each detected event is shared by the triggering anode stripe and, at most, one, of its neighbors [1]. The charge transport and signal generation simulations support this observation. Figure 2a shows the response of a single "pixel" to 122 keV photons from a ^{57}Co source. Note that the pulse heights of both anodes adjacent to the triggering stripe are summed and that nearly all events reside in the photopeak or fluorescence escape peak. The GEANT model also predicts nearly total energy deposit for the 122 and 136 keV photons of ^{57}Co with a fraction of fluorescence escape events similar to that measured. Figure 2b is the sum of the anode histograms from all 64 pixels and illustrates the good uniformity of response across the 8 × 8 stripe test region.

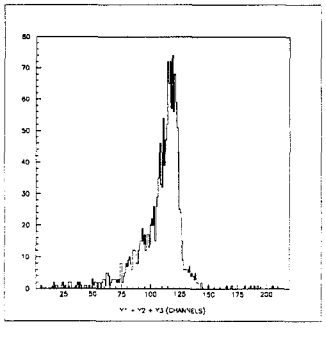

Fig. 2a. 122 keV single "pixel" spectrum

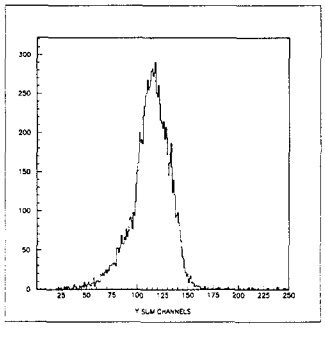

Fig. 2b. 122 keV sum spectrum of 64 "pixels."

B. *Imaging and spatial non-uniformity*

Figures 3 and 4 are images obtained from the 8 × 8 stripe (3 × 3 mm^2) test region of the prototype using 122 keV photons. The upper and lower images in each case are formed from the same data set. In the upper images event location is assigned to the stripe in each dimension recording the highest pulse height (0.375 mm pixels in each dimension). In the lower images event location is assigned based on interpolation of the pulse heights recorded by neighboring stripes (two pixels per stripe pitch, ~ 0.19 mm pixels in each dimension).

A gold aperture collimates a 170 μm diameter beam for the images shown in Fig. 3 a-b. Two tungsten foils were used to form the slits for the images shown in Fig. 4 a-b.

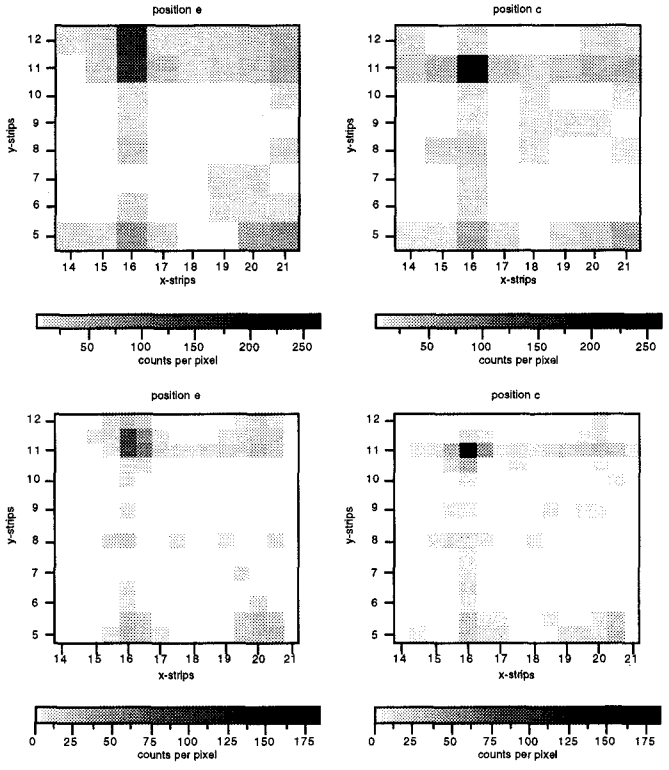

Fig. 3a. Image of 170 μm diameter 122 keV beam.

Fig. 3b. Same as 3a but beam moved 150μm in -*y* direction.

The lower images illustrate the advantage of recording the pulse heights of the triggering stripe and its neighbors for each event. Half-pitch resolution (~190 μm) event location capability is demonstrated in both dimensions. Note in figure 3b that the beam spot was moved 150 μm (0.4 × stripe pitch) in the -y direction from its position in figure 3a. This movement is more precisely represented by the finer resolution images. Note in Fig. 4b that the angle between the *x*-dimension stripes and the slit axis only becomes apparent in the finer resolution image.

The slit images also illustrate a non-uniform event location response. Such non-uniformities where neighboring pixels experience event rates that differ by as much as a factor of two across the imaging region are also seen under flood illumination conditions. Sweeping collimator beam studies show that events can be mislocated by as much as 50% of a stripe pitch (~190 μm). Our measurements indicate that events occurring between stripes are not lost but that the signal charge is preferentially collected by one of the neighboring stripes. In other words, the "reach" or effective widths of the individual stripes are not equal for this particular detector. This effect has also been reported in ref. [5].

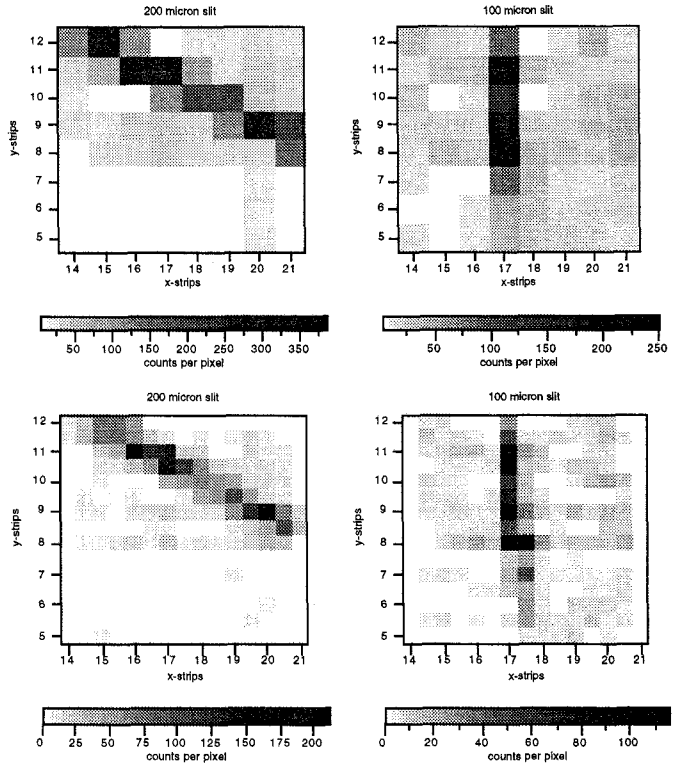

Fig. 4a . Image produced by a 200 μm wide slit.

Fig. 4b. Image produced by a 100 μm wide slit. Note slit tilt relative to *y*-axis.

Small bias differences between stripes may be responsible for some if not most of this non-uniformity. Figure 5 shows the discriminator trigger rate of eight consecutive anode stripes for three settings of the differential bias, applied independently, to stripe #8. Note that even a 1 Volt change in the differential bias results in a trigger rate change of >30% and that the neighboring stripes register a complementary change. Issues related to materials and contacts must also be considered in future investigations of the causes of spatial non-uniformities.

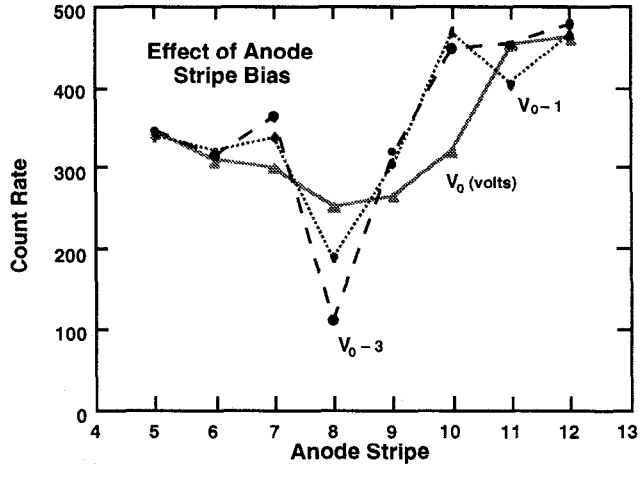

Fig. 5. Effect of small stripe bias differences.

C. Depth of interaction (z dimension)

Dramatic differences in the trigger rate and pulse height of cathode signals are observed when illuminating the detector from the top (cathode) and bottom (anode) sides. This is most apparent when using lower energy photons with a mean free path less than the detector thickness (1.5 mm). The pulse heights and thus the trigger rates of cathode signals are reduced for interactions occurring near the anode surface. Anode pulse heights and rates are relatively unaffected. This suggests that the ratio of cathode to anode pulse height can serve as a measure of the depth of interaction, i.e., the *z*-dimension.

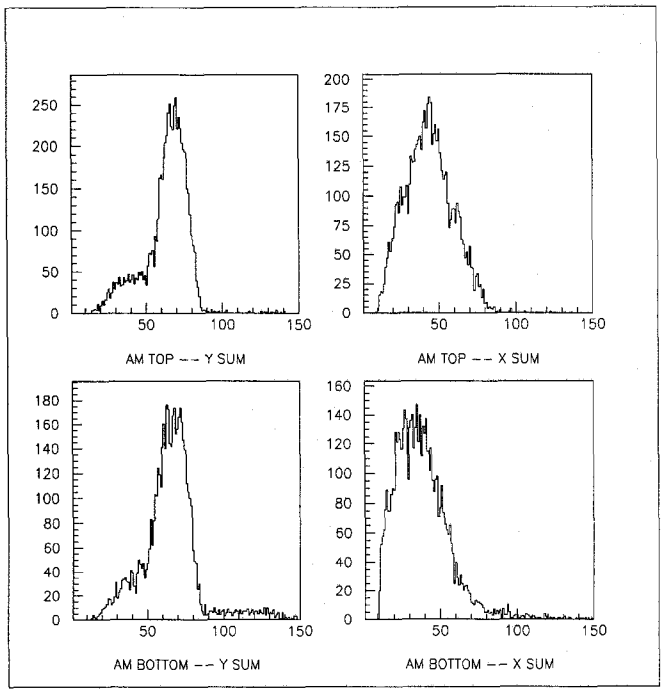

Fig. 6. Anode and cathode pulse heights; top and bottom 60 keV illuminations.

Figure 6 contains four histograms of the sums of anode and cathode pulse heights recorded for each event for flood illumination runs of the 8 × 8 stripe, 64 "pixel," test region of our prototype using a ^{241}Am (60 keV) source. The photon mean free path at 60 keV is 0.26 mm. The anode pulse height distributions are shown on the left; the cathode distributions on the right. The top (bottom) figures show the results when illuminating the detector from the top (bottom) or cathode (anode) side. Note that lower cathode pulse heights are observed for bottom illumination while the anode pulse heights are relatively unaffected. The implication for the efficiency of strip detectors is discussed below.

D. Measurements of detection efficiency, sensitive depth vs. energy

To determine the event detection efficiency the predicted count rate was compared to that measured. Parameters used to determine the predicted counting rate include the following: the source activity and line strength, the solid angle subtended by the source on the active area of the detector, and the energy

dependent photon interaction rate in the detector. From these measurements we concluded that while anode event detection is nearly 100%, cathode and therefore coincident event detection is decidedly less than 100% and is energy and location dependent.

In the following discussion we normalized the efficiency to the anode trigger rate and defined it to be the ratio of detected coincident counts per unit area to detected anode counts per unit area. We measured efficiencies for several photon energies. Our observations indicate that as interactions occur closer to the anode, the signal detected on an individual cathode stripe becomes so small that the discriminator threshold (~15 keV equivalent) is not reached and the event is not detected. This behavior is qualitatively predicted by the model. Based on the assumption that events occurring beyond a certain depth from the cathode are not detected, we computed an effective depth from the measured efficiency. The results are shown and compared with the photon mean free path in figure 7.

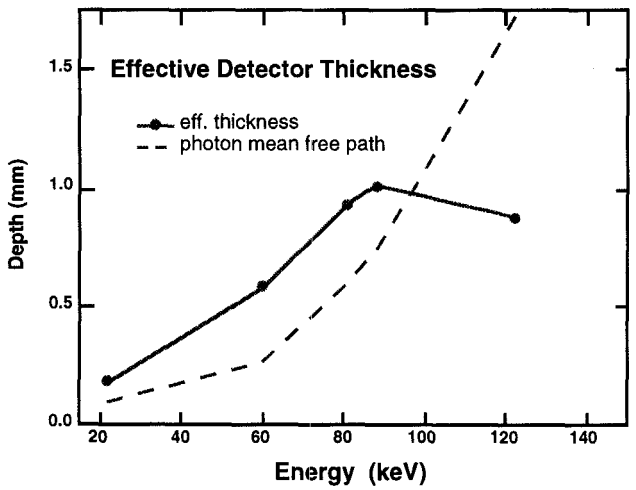

Fig. 7. Effective detector thickness vs. photon energy. Illumination is from cathode side.

In the lab the fast signals must surpass the discriminator threshold in order for an ADC strobe to be produced and the event to be registered. The effective thickness will be increased if the readout electronics permit the setting of lower cathode thresholds. Other tests in the lab indicate the efficiency advantage of summing the fast cathode signals prior to discrimination or of employing detectors fabricated with a coarser cathode pitch.

The results from the simulations are shown in figure 8. The simulated pulse heights of fast cathode and anode signals are plotted as a function of two parameters. The first parameter is vertical distance from the anode. For the cathodes the further the interaction point is from the cathode, the smaller the amplitude of the cathode signal. A depth effect is also apparent for the anodes but it is not as dramatic as that predicted for the cathodes particularly in the sensitive region of the detector near the cathode surface. The second parameter is lateral distance from the center of the electrode stripe.

Events occurring directly below the center of an electrode have a larger amplitude than events occurring in the gap between electrodes. Note that the simulation predicts essentially linear charge sharing of the signal with the neighboring electrode for events occurring between electrodes.

E. Relative signal timing (anode/cathode)

A time-to-amplitude converter (TAC) was employed to measure the arrival time of the cathode signal relative to that of the anode. Figure 9 is a histogram of the TAC output for flood illumination events of the 8 × 8 stripe test region with a 122 keV source. The cathode signals stop the TAC and no late stops are present as would be expected from the late arrival of holes several μs after the electrons are collected on the anodes. The measured FWHM of 270 ns is consistent with the timing spread expected when using level discriminators for the timing of signals with ~ 200 ns rise times.

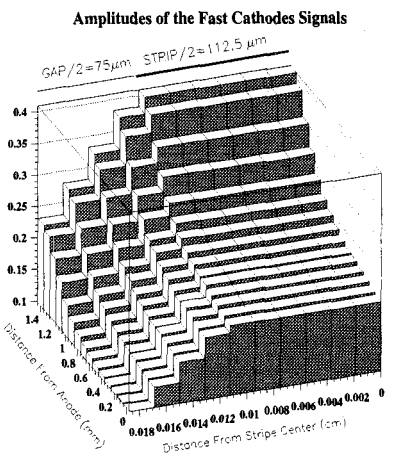

Fig. 8a.
Cathode signal simulation

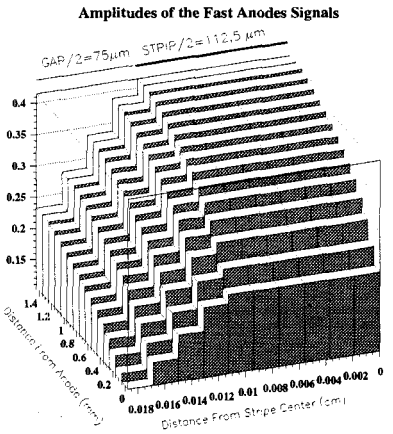

Fig. 8b.
Anode signal simulation

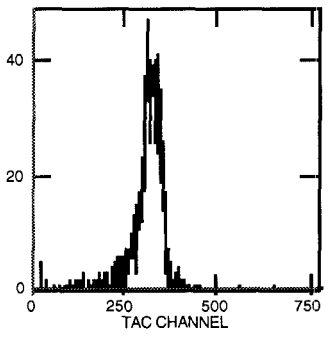

Fig. 9. Relative cathode-anode signal arrival time. FWHM = 270 ns.

The arrival of cathode and anode signals is essentially simultaneous for the vast majority of *x-y* coincident events from 20 keV to 662 keV. Although signal shapes and rise times vary from event to event, simultaneous arrival of cathode and anode signals is also observed for the vast majority of events when using a digital oscilloscope to view the charge sensitive preamp outputs. However, the model predicts a larger hole component of the cathode signal arriving as late

as 2 μs after the anode signal for events occurring nearer the anode. This is not observed in these laboratory tests.

V. Comparison of Measurements and Simulations

The model qualitatively predicts many of the observations and trends seen in the data: nearly total energy deposit in the detector at 122 keV, a reduction of signal on a given electrode and the sharing of the signal with the neighboring stripe when the interaction occurs between electrodes, and a reduction of cathode pulse height with increasing depth or distance from the cathode. Attempts at comparing the efficiency measurements and simulations indicate that the model predicts higher efficiencies than those that are measured.

The simultaneous arrival of signals indicates that electron transport is the dominant component of the detected signals at the cathodes as well as the anodes, whereas the model predicts a larger influence of the hole component for the cathode signals and, to a lesser extent, for the anode signals. These discrepancies suggest that some of the material transport properties must be modified in the model.

VI. Conclusions and Future Work

Sub-pitch spatial resolution (~190 μm) in two dimensions and good energy resolution and spectral uniformity have been demonstrated with this prototype. The spatial response is, however, non-uniform as interactions can be mislocated by as much as 50% of a stripe pitch (~190 μm). Small stripe bias differences represent a likely source of this non-uniformity. We are considering alternate biasing schemes for future testing. The ratio of cathode to anode pulse height can be an indicator of the third dimension, the depth of the interaction, although further tests using collimated sources are necessary to separate the depth effects from the lateral location effects predicted by the model. We also plan to investigate the spectroscopic advantages of depth related pulse height corrections. Depth effects, particularly apparent for cathode signals, are exploited to compute an energy dependent sensitive thickness for the strip detector prototype in its present test configuration. The ability to set lower discriminator thresholds, particularly for the cathode stripes will improve the efficiency. Coarser cathode stripe pitch and signal summing prior to level discrimination will also help. We will be conducting additional studies in this area.

A model that includes the photon interaction, carrier transport and the electronics has been developed that qualitatively reproduces the measurements but still lacks the quantitative agreement that is sought. While measurements indicate that signals are dominated by electrons, the simulation predicts larger hole components on both cathode and anode signals. Further measurements of the CdZnTe transport properties might help resolve these discrepancies.

We plan to measure these properties with this detector in a series of dedicated experiments by scanning the anode and cathode planes with a collimated α-source. Simultaneously recorded charge signals from many anode and cathode stripes will directly measure the electron and hole transit times, and therefore the mobilities, and impose stringent constraints on the trapping and detrapping coefficients and the field profile.

VII. Acknowledgments

This work is supported by NASA's High Energy Astrophysics Gamma Ray Astronomy Research and Analysis program and by the Natural Sciences and Engineering Research Council of Canada.

VIII. References

[1] J.M. Ryan et al., "Large Area Sub-Millimeter Resolution CdZnTe Strip Detector for Astronomy," SPIE Conf. Proc., San Diego, vol. 2518 (July 1995) 292.

[2] J.R. Macri, et al., "Development of an Orthogonal-Stripe CdZnTe Gamma Radiation Imaging Spectrometer," IEEE Trans. Nucl. Sci., vol. 43, no. 3 (June 1996) 1458.

[3] H.B. Barber, et al., "CdZnTe arrays for nuclear medicine imaging," in Proceedings, SPIE, Denver, CO, vol. 2859 (August 1996) 26.

[4] J.R. Macri et al., "Progress in the development of large area sub-millimeter resolution CdZnTe strip detectors," in Proceedings, SPIE, Denver, CO, vol. 2859 (August 1996) 29.

[5] J.L. Matteson, et al., "CdZnTe strip detectors for high-energy x-ray astronomy," in Proceedings, SPIE, Denver, CO, vol. 2859 (August 1996) 58.

[6] C.M. Stahle, et al., "CdZnTe strip detector for arcsecond imaging and spectroscopy," in Proceedings, SPIE, Denver, CO, vol. 2859 (August 1996) 74.

[7] L.A. Hamel, et al., "Signal Generation in CZT Strip Detectors," IEEE Trans. Nucl. Sci., vol. 43, no. 3 (June 1996) 1422.

[8] J.D. Eskin, et al., "The effect of pixel geometry on spatial and spectral resolution in a CdZnTe imaging array," in Conference Record, IEEE NSS, San Francisco, CA (October 1995) 544.

[9] L.A. Hamel, et al., "Charge transport and signal generation in CdTe pixel detectors", in Proceedings, 9th International workshop on room temperature semiconductor X and g-ray detectors, Grenoble, (September 1995).

[10] L.A. Hamel, "Signal induced in semiconductor detectors with a linear field profile in the presence of trapping and detrapping", submitted to Nucl. Instr. and Meth. A.